# CITRUS GREENING DISEASE DETECTION USING AIRBORNE MULTISPECTRAL AND HYPERSPECTRAL IMAGING

**A. Kumar**
*Electrical and Computer Engineering*
*University of Florida*
*Gainesville, Florida*

**W. S. Lee**
*Agricultural and Biological Engineering*
*University of Florida*
*Gainesville, Florida*

**R. Ehsani and L. G. Albrigo**
*Citrus Research and Education Center*
*University of Florida*
*Lake Alfred, Florida*

**C. Yang and R. L. Mangan**
*Kika de la Garza Subtropical Agricultural Research Center*
*USDA ARS*
*Weslaco, Texas*

## ABSTRACT

Hyperspectral imaging can provide unique spectral signatures for diseased vegetation. Airborne hyperspectral imaging can be used to detect potentially infected trees over a large area for rapid detection of infected zones. Ground inspection and management can be focused on these infected zones rather than entire grove, making this less labor intensive and time consuming. This paper proposes a method to detect the citrus greening disease (Huanglongbing or HLB) infected areas in citrus groves using airborne hyperspectral and multispectral imaging. This would prevent further spread of infection, if complimented by development of efficient management plans of infected areas. Hence, airborne hyperspectral imaging would provide much faster results over a wide range of area. An aerial hyperspectral image with a spectral range of 457-921 nm spanning across 128 spectral bands was acquired from an HLB infected citrus grove in Florida in December 2009. The imagery had a 3.6 nm spectral resolution and 1 m spatial resolution. A multispectral image with 4 bands (red, green, blue, and NIR) spanning across a spectral range of 480-830 nm with 40 nm bandwidth was also acquired from the same grove. Polymerase chain reaction (PCR) test based ground truthing of this area had been carried out where the infected tree coordinates were recorded. An image derived spectral library was built using the

above images and categories of Healthy and HLB infected pixels were created based on the PCR results and locations of the infected trees. Ground measurements were obtained for Healthy and HLB infected citrus trees from the same grove along with their degrees of infection. A hyperspectral imaging software (ENVI, ITT VIS) was used for the analysis of these images. HLB infected areas were identified using image-derived spectral library, the mixture tuned match filtering (MTMF), the spectral angle mapping (SAM), and linear spectral unmixing (LSU). It was seen that accuracy of MTMF method was greater than the other methods. The accuracy of SAM using multispectral images was comparable to the results of the MTMF and also gave higher accuracy when compared to SAM analysis on hyperspectral images.

**Keywords:** Aerial, Citrus, Greening, Ground truthing, Hyperspectral, Multispectral, Spectral library.

## INTRODUCTION

Citrus greening disease, also known as Huanglongbing (HLB) or yellow dragon disease, is thought to have originated from China in the early 1900s. The disease is primarily spread by two species of psyllid insects. The disease in Florida is caused by a bacterium, Candidatus Liberibacter asiaticus, that is transmitted by a tiny insect, the Asian citrus psyllid (Diaphorina citri), which thrives on young citrus leaves. The Asian citrus psyllid has been present in Florida since 1998 (FDACS DPI, 2006). There are three strains of the bacteria, an Asian, an African version and an American strain discovered in Brazil (Garnier et al., 2000). The Asian strain, Candidatus Liberibacter asiaticus was found in Florida in early September, 2005. The bacteria itself is not harmful to humans but the disease has harmed trees in Asia, Africa, the Arabian Peninsula, and Brazil (Brlansky et al., 2005) as it obstructs the flow of nutrients in citrus trees.

HLB is now considered to be one of the most destructive and devastating of all citrus diseases and is now a major threat to the $9 billion Florida citrus industry. The HLB infected trees die within 3-5 years and there is no known cure. The infected trees have to be removed and destroyed. As of February 2010, citrus trees in 3,122 different sections (square mile) in 34 counties were infected in Florida (FDACS, DPI, 2010). Growers urgently need diagnostic tools for early detection, because infected trees may not show symptoms for months or years, during which they are contagious. Current molecular diagnostic tests do not detect the disease soon enough to stop its spread. These methods have proved inadequate and many farmers are not replanting, because young, vigorous trees attract the psyllids. Citrus plants infected by the citrus greening bacteria may not show symptoms for years following infection. As the bacteria move within the tree, the entire canopy progressively develops a light green or yellow color (Fig. 1). The most characteristic symptoms of citrus greening are a blotchy leaf mottle and vein yellowing that develop on leaves attached to shoots showing the overall yellow appearance. Infected trees produce fruits which are unmarketable. On Mandarin orange, fruit may develop an uneven ripening such that they appear half orange and half yellow. This symptom is the origin of the common name “greening”.

**Fig. 1. An HLB infected citrus tree**.

Culturing and sequencing the genome of the greening pathogen and the host would facilitate studies of interactions between the host, the bacteria and the insect that acts as a carrier or vector of the disease (Tian et al., 1996). This would aid in development of diagnostic tools that would enable early detection of infected trees. Until such tools are available, there is a critical need to find ways which can detect HLB infected areas within citrus groves and also monitor newly infected areas. A PCR method can be used to confirm infections of HLB, but the process is expensive and hence not feasible and economical for larger areas. Moreover, time consuming and labor intensive ground-based inspection methods are not suitable for identifying all individual tree infections over a larger area.

Hyperspectral imaging can provide unique spectral signatures, and thus can be used to detect potentially infected trees over a large area for rapid detection of infected zones, where ground inspection and management should be focused. This will significantly reduce the cost of surveying as well as monitoring new areas for infection and also provide faster results.

Hyperspectral reflectance imaging has been successfully used to identify disease, nutrient and water deficiencies and defects in different fruits and vegetables. A spectral information divergence based image classification method provided useful means for detecting canker lesions on citrus fruit (Qin et al., 2008). A significant problem was that greasy spot, insect damage, and melanose had similar reflectance properties to canker, and the chances for misclassifying these three diseases were higher than other kinds of peel conditions. The reflectance spectra from the hyperspectral images of apples were used to find the optimal wavelengths to discriminate the defect region from the normal region (Lee et al., 2005). Rice canopy hyperspectral reflectance has been used to detect bacterial leaf blight (BLB) by establishing spectral models for assessing disease severity for future site-specific management (Yang, 2009). Hyperspectral images in the range from 339 to 1014 nm were used to detect disease during early stages of lettuce growth (Matsuo et al., 2006). It has been observed that plants under stress induced by a disease, based on the severity of the infection, tend to absorb more light in the near infrared (NIR) region.

The overall objective of this study was to develop a method to detect HLB infected areas in citrus groves using airborne hyperspectral imaging which will enable more rapid detection of potentially infected areas. This coupled with development of efficient management plans of these areas will therefore prevent further spread of the infection.

## MATERIALS

### The hyperspectral and multispectral images

The citrus grove chosen for this study was located in the Collier County in Florida, USA and is spread across 77.37 acres. The center coordinates of this location were 26° 21' 12.27" N and 81° 21' 15.76" W. One multispectral and a hyperspectral image were acquired from both blocks marked E1 (Fig. 2). The grove contained Valencia oranges.

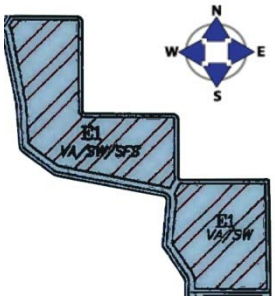


**Fig. 2. The Citrus grove site under study (Summerland Grove – Consolidated Citrus limited Partnership). Scale: 1cm = 192 m.**

A high resolution airborne four-camera imaging system (Yang, 2010) and a hyperspectral imaging system (Yang et al., 2003) were used for image acquisition in this study. The multispectral system acquired 12-bit images with 2048 × 2048 pixels in blue (430-470 nm), green (530-570 nm), red (630-670 nm), and near-infrared (NIR) (810-850 nm) bands. The CCD based hyperspectral sensor captured 128-band images covering a spectral range from 457.2 to 921.7 nm at 3.63 nm intervals. The image swath was 640 pixels and the radiometric resolution was 12 bit. The multispectral image was acquired at an altitude of 3,048 m, while the hyperspectral image was acquired at 1,524 m. Both images were georeferenced to the UTM coordinate system with zone 17N projection with the datum of WGS-84, and resampled to 1 m pixel resolution. The images were spectrally uncalibrated and the digital numbers (DN) on the imagery were represented using 12 bit numbers, ranging from 0 to 4095.

### Ground measurements at the site under study

In-field measurements were obtained from the study site using a portable hand-held spectrometer (HR-1024, Spectra Vista Corporation, Poughkeepsie, NY) for four different categories of trees in the grove. The categories were HLB1 (tree canopy infected in some areas), HLB2 (HLB infected tree in general decline),

nutrient deficient (but no HLB infection), and healthy tree. The ground spectrometer recordings spanned across 348 nm to 2300 nm with a 3 nm spectral resolution.

The PCR based ground truthing for confirming HLB infection was also conducted for trees in the study site. The ground truthing was carried out by recording locations of infected trees using an RTK GPS receiver (HiPer XT, Topcon, Olathe, KS).

## METHODS

### Spectral library construction

Pixel spectra were collected from both the hyperspectral and the multispectral image corresponding to the locations recorded for each of the categories mentioned in the ground measurements. The pixel spectra for each tree flagged under various categories in the ground measurement was collected and there were a total of 49 observations for HLB1, 20 observations for HLB2, 24 nutrient deficient and 11 healthy tree spectra.

Pixel spectra were collected for the trees which were confirmed HLB positive and those declared healthy based on the PCR results. Using the PCR tests, a total of 30 HLB infected trees were identified and their corresponding pixel spectra were collected from the hyperspectral and multispectral image.

### Data analysis and pixel detection

A total of 20 infected pixel spectra, 10 pixels each from both the E1 blocks of the citrus grove formed a training set of the image derived spectral library. The rest of the 10 pixels formed a validation set of spectral library against which detection accuracy of the image analysis would be documented. Endmember detection algorithms like spectral angle mapper (SAM), mixed tuned matched filtering technique (MTMF) and spectral unmixing were applied on hyperspectral and multispectral images.

## RESULTS AND DISCUSSION

### Spectral data analysis from ground measurements

The portable spectrometer readings for all the data points from the citrus grove site were plotted. Fig. 3 shows the difference in the spectral characteristics of the tree categories classified. Both categories of HLB show higher reflectance in visible region compared to both nutrient deficient and healthy trees. The data corresponding to the range 1800-2000 nm was found noisy and hence removed from the plot.

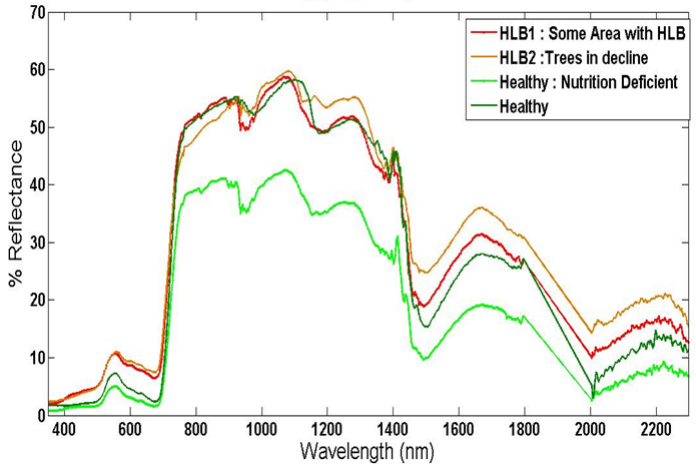


**Fig. 3. A portable handheld spectrometer was used to measure in-field reflectance spectra of HLB infected (HLB1 and HLB2), nutrient deficient trees and healthy canopies. The spectra for HLB1, HLB2, nutrient deficient, healthy are the average of 49, 20, 24 and 11 spectral measurements, respectively.**

**Pixel data analysis from hyperspectral and multispectral images**

The trees corresponding to which ground measurement was recorded was marked on the hyperspectral and multispectral images. The corresponding pixel spectra of these data points from hyperspectral and multispectral images is shown in Fig. 4 and Fig. 5, respectively. It can be seen that the DN (digital number) value for HLB1 is higher than the Healthy tree category in both the hyperspectral and multispectral images. This is consistent with spectral plot of in-field reflectance measurements.

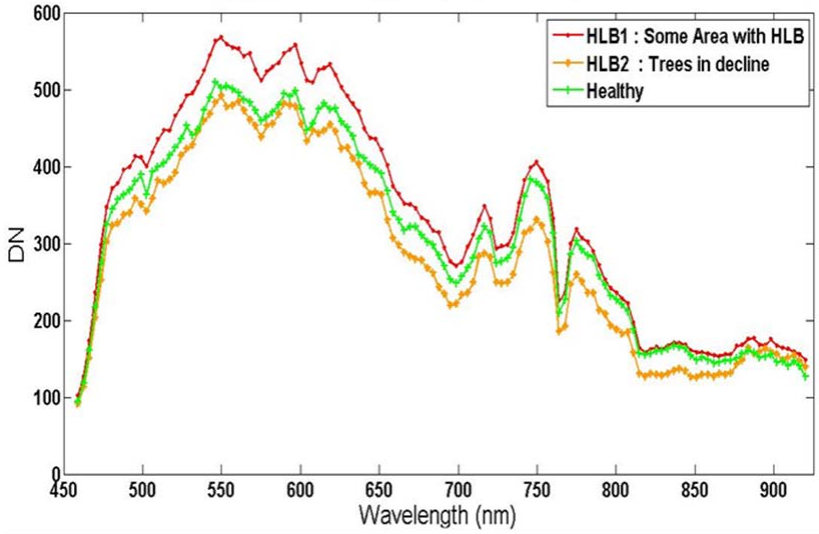


**Fig. 4. Spectral plot of HLB infected (HLB1 and HLB2) and healthy canopies corresponding to trees in ground measurement in Fig. 3 for Hyperspectral image. The spectra for HLB1, HLB2 and Healthy are the average of 49, 20 and 11 pixel spectra, respectively.**

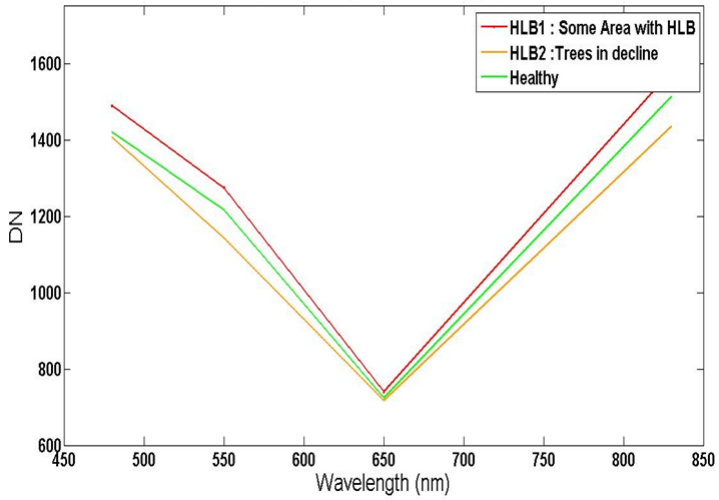


**Fig. 5. Spectral plot of HLB infected (HLB1 and HLB2) and healthy canopies corresponding to the trees in ground measurement in Fig. 3 for multispectral image. The spectra are the average of same number of data points as in Fig. 4 for each category.**

The PCR test confirmed HLB and Healthy trees from both the image sites. The trees corresponding to this ground truthing data were located and their pixel spectra were plotted for both hyperspectral and multispectral images, shown in Fig. 6 and Fig. 7, respectively.

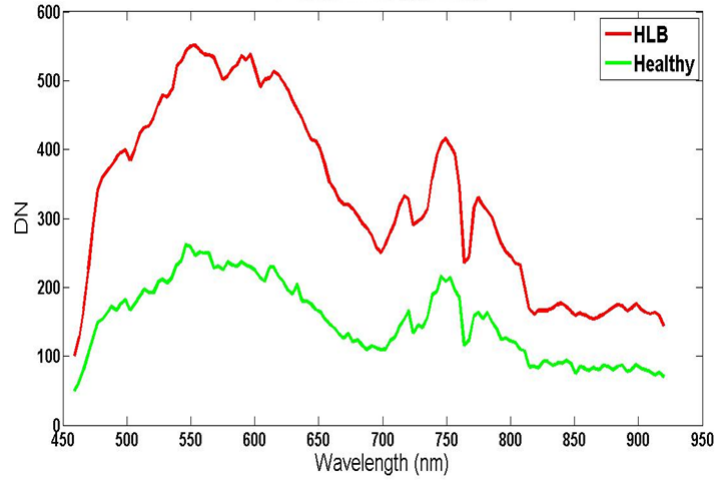


**Fig. 6. Spectral plot of PCR test confirmed HLB infected and Healthy tree pixel in the hyperspectral image. Each spectrum is an average of 15 observations points.**

Both Fig. 6 and Fig. 7 show a higher DN value for HLB infected pixels corresponding to their Healthy counterpart. This result is again consistent with the reflectance measurements using hand-held spectrometer at the grove site.

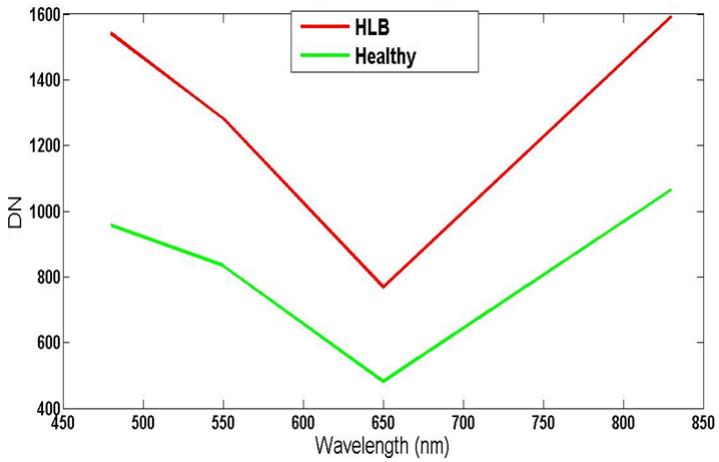


**Fig. 7. Spectral plot of PCR test confirmed HLB infected and Healthy tree pixel in the multispectral image. Each spectrum is an average of 15 observations points.**

**Detection of HLB infected pixel in hyperspectral and multispectral images**

**Method-1: Spectral Angle Mapper (SAM)**

SAM analysis used the existing image derived spectral library created from 30 pixels each for both categories (healthy and HLB infected) confirmed using PCR tests. Multiple maximum spectral angles were used for the SAM algorithm for mapping pixels. Spectral angle of 0.1 was used for the entire endmember collection of healthy pixels. An angle of 0.05 was used for the diseased pixel endmembers and it was found to give optimum results for both E1 sites in the hyperspectral image. Fig. 8 documents the steps involved in the SAM analysis.

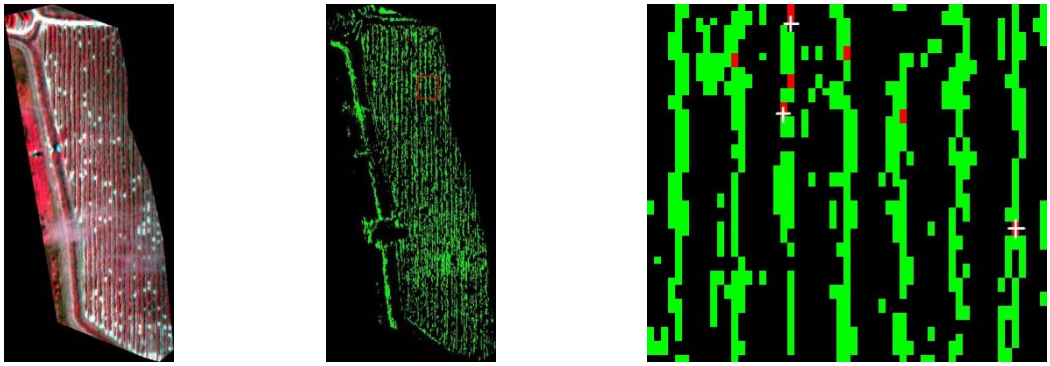


**Fig. 8. SAM procedure applied on E1 (west grove site): (a) Original hyperspectral CIR image, (b) SAM result of the image with spectral angle 0.1 for the healthy pixels and 0.05 for the HLB infected pixels. Green pixel is healthy vegetation and red pixel was identified as HLB infected pixels, (c) The white cross-hair on the enlarged rectangular subsection of (b) indicates ground truth location for infected trees.**

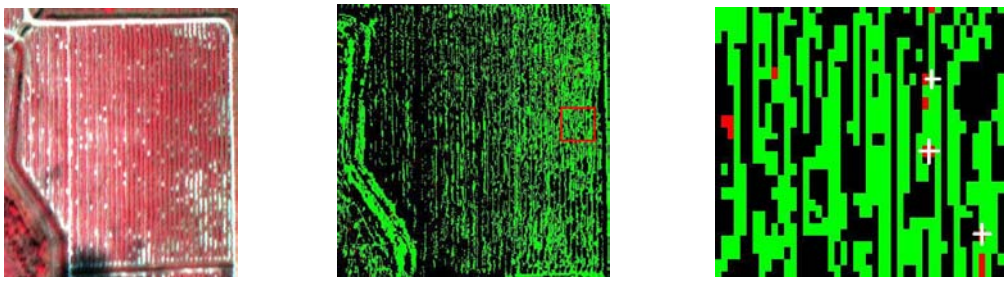

(a) (b) (C)

**Fig. 9. SAM procedure applied on E1 (east grove site): (a) Original hyperspectral CIR image, (b) SAM result of the image with spectral angle 0.1 for the healthy pixels and 0.05 for the HLB infected pixels. Green pixel is healthy vegetation and red pixel was identified as HLB infected pixels, (c) The white cross-hair on the enlarged rectangular subsection of (b) indicates ground truth location for infected trees.**

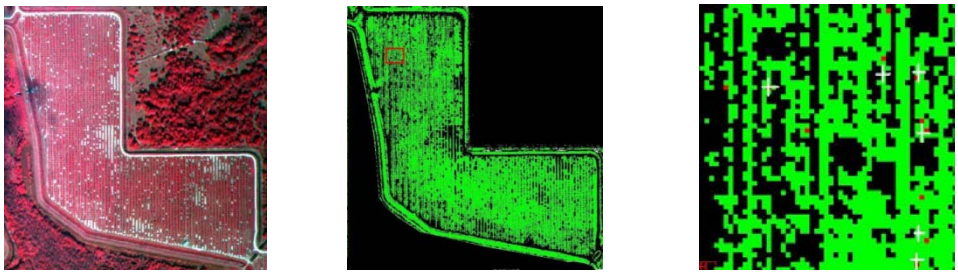

(a) (b) (C)

**Fig. 10. SAM procedure applied on E1 (west grove site): (a) Original multispectral CIR image, (b) SAM result of the image with spectral angle 0.1 for the healthy pixels and 0.04 for the HLB infected pixels. Green pixel is healthy vegetation and red pixel was identified as HLB infected pixels, (c) The white cross-hair on the enlarged rectangular subsection of (b) indicates ground truth location for infected trees.**

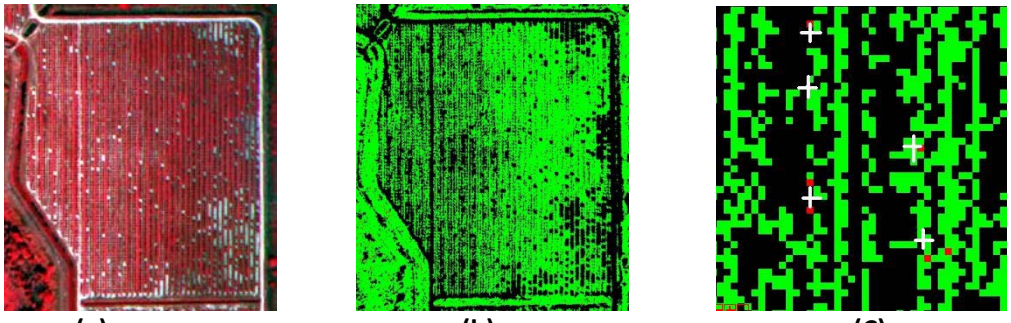

(a) (b) (C)

**Fig. 11. SAM procedure applied on E1 (east grove site): (a) Original multispectral CIR image, (b) SAM result of the image with spectral angle 0.1 for the healthy pixels and 0.04 for the HLB infected pixels. Green pixel is healthy vegetation and red pixel was identified as HLB infected pixels, (c) The white cross-hair on the enlarged rectangular subsection of (b) indicates ground truth location for infected trees.**

The corresponding spectral library for multispectral images was used while carrying out the SAM analysis on both multispectral image sites. A spectral angle of 0.1 was used for the entire endmember collection of healthy pixels and an angle of 0.04 was used for the diseased pixel endmembers. This was found to give optimum results for both E1 sites in the multispectral image.

Let us consider the set SAM_HLB as the collection of pixels (trees) detected as HLB infected and PCR_HLB as the set of all PCR confirmed HLB pixels (trees) within the site. The intersection of these two sets SAM_PCR_HLB would be an estimate of the accuracy of the SAM detection method. Table 1 estimates the detection accuracy of SAM analysis result. Pixels detected as infected are validated against the PCR confirmed ground truthing data. HS and MS stands for hyperspectral and multispectral images, respectively.

Table 1. SAM accuracy table.

| Site | Image type | SAM_HLB | PCR_HLB | SAM_PCR_HLB | Accuracy (%) |
|---|---|---|---|---|---|
| E1 - West | HS | 52 | 15 | 9 | 60.0 |
| E1 - East | HS | 95 | 15 | 10 | 66.6 |
| E1 - West | MS | 83 | 15 | 12 | 80.0 |
| E1 - East | MS | 143 | 15 | 13 | 86.6 |

**Method-2: Mixed tuned match filtering (MTMF) procedure**

This following method was applied on both the hyperspectral images for the east and west grove site (E1). The minimum noise transform (MNF) was applied to the raw image data to create MNF bands. This segregates valuable spectral information and undesirable noise. Lower MNF bands contain most of the spectral information and higher MNF bands can be discarded as it contains most of the image data noise. The existing image derived spectral library for hyperspectral images is used by the MTMF on the MNF transformed image to match the HLB infected endmember spectra as shown in Fig. 12 and Fig. 13.

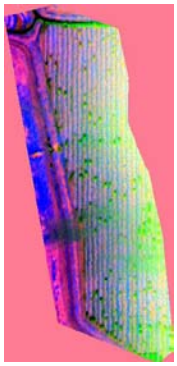

(a)

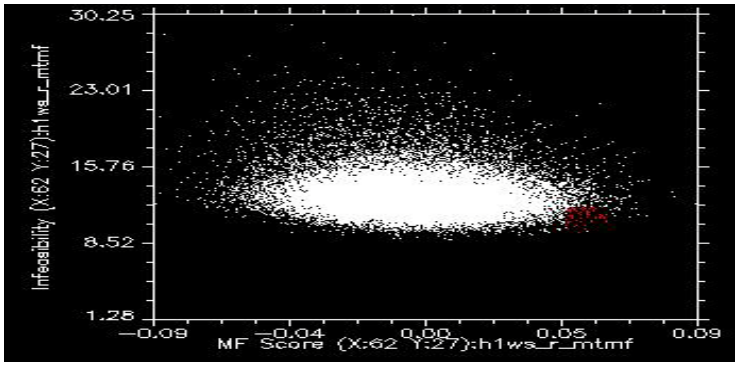


(b)

(c) (d)

**Fig. 12. MTMF technique applied on E1 (west grove site): (a) MNF RGB image (retains all spectrally pure pixels), (b) 2D scatter plot of pixels after MTMF is carried out on (a). A low infeasibility and high MF score indicated better match to the endmember spectra (HLB pixels) being detected. These pixels have the color red in the scatter plot, (c) Target endmember (HLB pixels) projected on the MTMF output image as red pixels, (d) The white cross-hair on the enlarged rectangular subsection of (c) indicates ground truth location for infected trees.**

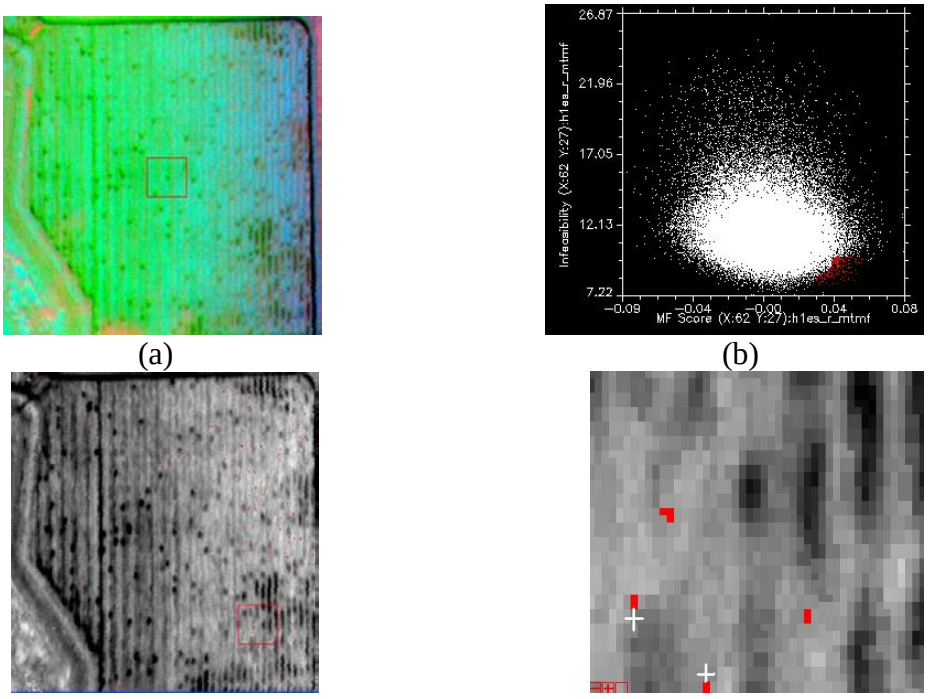


(a) (b)

(c) (d)

**Fig. 13. MTMF technique applied on E1 (east grove site): (a) MNF RGB image. (Retains all spectrally pure pixels), (b) 2D scatter plot of pixels after MTMF is carried out on (a). A low infeasibility and high MF score indicated better match to the endmember spectra (HLB pixels) being detected. These pixels have the color red in the scatter plot, (c) Target endmember (HLB pixels) projected on the MTMF output image as red pixels, (d) The white cross-hair on the enlarged rectangular subsection of (c) indicates ground truth location for infected trees.**

Let us consider the set MTMF_HLB as the collection of pixels (trees) detected as HLB infected. The intersection of the sets PCR_HLB and MTMF_PCR_HLB would be an estimate of the accuracy of the MTMF detection method. Table 2 estimates the detection accuracy of MTMF analysis result. Pixels detected as infected are validated against the PCR confirmed ground truthing data.

Table 2. MTMF accuracy table.

| Site | Image type | MTMF_HLB | PCR_HLB | MTMF_PCR_HLB | Accuracy (%) |
|---|---|---|---|---|---|
| E1 - West | HS | 78 | 15 | 11 | 73.3 |
| E1 - East | HS | 126 | 15 | 12 | 80.0 |

**Method-3: Linear Spectral Unmixing (LSU) method**

Spectral unmixing method was applied on both the hyperspectral images for the east and west grove site (E1). The Minimum noise transform (MNF) was applied to the raw image data to create MNF bands to obtain spectrally pure pixels. Spectral unmixing procedure is applied on the MNF data. This technique finds the abundance of the endmember spectra (HLB infected pixels provided as input using the spectral library) in each reference spectra of the MNF image. Detection of HLB infected pixels is achieved using a high threshold on the abundance value of the unmixed output pixels indicating a better match to endmember spectra as shown in Fig. 14.

(a) (b)

**Fig. 14. Spectral unmixing method applied on E1 (west grove site). (a) Spectral unmixing applied on MNF transformed image of Fig. 12(a). Red pixels indicate infected trees which were matched based on high abundance threshold value. (b) The white cross-hair on the enlarged rectangular subsection of (a) indicates ground truth location for infected trees.**

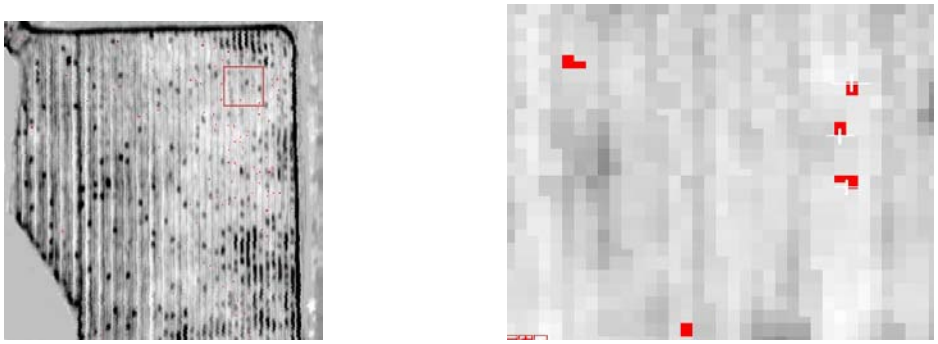

(a) (b)

**Fig. 15. Spectral Unmixing method applied on E1 (east grove site). (a)_Spectral unmixing applied on MNF transformed image of Fig. 13(a). Red pixels indicate infected trees which were matched based on high abundance threshold value. (b) The white cross-hair on the enlarged rectangular subsection of (a) indicates ground truth location for infected trees.**

Let us consider the set LSU_HLB as the collection of pixels (trees) detected as HLB infected. The intersection of the sets PCR_HLB and LSU_PCR_HLB would be an estimate of the accuracy of the LSU detection method. Table 3 estimates the detection accuracy of LSU analysis result. Pixels detected as infected are validated against the PCR confirmed ground truthing data.

Table 3. LSU accuracy table.

| Site | Image type | MTMF_HLB | PCR_HLB | MTMF_PCR_HLB | Accuracy (%) |
|---|---|---|---|---|---|
| E1 - West | HS | 69 | 15 | 8 | 53.3 |
| E1 - East | HS | 143 | 15 | 11 | 73.3 |

It was seen that E1- west site accuracy results were lower than the east site for all the above methods. E1-west site consisted of 32 rows of trees, out of which only 12 tree rows could be used for hyperspectral data processing. The other parts of the image were unavailable due to poor quality and interference of cloud clusters. As a result, ground information and PCR results of only the first 12 rows could be utilized in the spectral library construction. This could explain the variation in the accuracy results in the west and east grove site.

The accuracy results are strictly based on the intersection of the two sets, the PCR_HLB and the set of all trees detected as infected by the detection method. The PCR results are not available for every tree in the grove, as conducting such a comprehensive test on the grove site would be extremely time consuming and costly. Having more number of positive PCR results increases the size of the set PCR_HLB which would provide a better estimate of the accuracy, since the intersection of the two sets is bound to increase or decrease based on the performance of the method.

Since the status of every tree on the grove was not known, quantizing the false positives (Healthy tree identified as infected) was not possible. This would have provided an even better representation and accuracy of the results.

## CONCLUSION

An aerial hyperspectral image with a spectral range of 457-921 nm with 128 spectral bands, 3.6 nm spectral resolution, 1 m spatial resolution and a 4 band multispectral image with a spectral range of 480-830 nm with 40 nm bandwidth were used to detect HLB infected trees. The mixture tuned match filtering (MTMF), the spectral angle mapper (SAM) and linear spectral unmixing (LSU) methods were used for this purpose. Polymerase chain reaction (PCR) test based ground truthing of selected trees in the area had been carried out to determine the status of these trees and classifying them into healthy or infected. These observations were used for spectral library construction as well as validation and accuracy estimation of results. Ground measurements with hand-held spectrometer were also obtained for Healthy and HLB infected citrus trees from the same grove site along with their degrees of infection. This was used as an alternative to PCR results for result validation.

A fairly high detection accuracy of 80% was achieved using MTMF on hyperspectral image of the E1- east site. SAM with multispectral images also gave a very high accuracy rate (87%). The E1-west site observed lower detection accuracy compared to the east site. This was due to the fact that the hyperspectral image was cropped due to poor quality and hence all ground measurements for this site could not be utilized as all tree rows were not available for hyperspectral image processing. A better estimate of accuracy can be achieved with more PCR results and a comprehensive ground survey. This would help in the quantization of false positives in the result.

## ACKNOWLEDGEMENT

The authors would like to thank Dr. Eran Raveh, Ms. Sherrie Buchanon, Ms. Ujwala Jadhav, Mr. Ashish Mishra and Mr. Eduardo Chica for their assistance in this study.

## REFERENCES

Brlansky, R. H., K. R. Chung, M. E. Rogers. 2005. 2006 Florida citrus pest management guide: Huanglongbing (citrus greening). UF/IFAS Extension.

FDACS DPI. 2006. Huanglongbing (HLB)/citrus greening disease. Available at www.doacs.state.fl.us/pi/chrp/greening/citrusgreening.html. Accessed 7, Sep. 2006.

FDACS DPI. 2010. Disease detection maps: Known distribution of citrus canker/citrus greening (HLB) in Florida. http://www.doacs.state.fl.us/pi/chrp/ArcReader/ArcReader.html. Accessed April 6, 2010.

Lan, Y., Y. Huang, W. C. Hoffmann. 2007. Airborne Multispectral remote sensing with ground truth for areawide pest management. ASABE Paper No. 073004. St. Joseph, Mich.: ASABE.

Lee, K., S. Kang, M. S. Kim, and S. Noh. 2005. Hyperspectral imaging for detecting defect on apples. ASAE Paper No. 053075. St. Joseph, Mich.: ASABE.

Lee, W. S., R. Ehsani, and L. G. Albrigo. 2008. Citrus greening (Huanglongbing) detection using aerial hyperspectral imaging. In the Proceedings of the 9th International Conference on Precision Agriculture, Denver, Colorado.

Matsuo, K., M. Iwate, K. Nishiwaki, S. Zhang, and M. Yashiro. 2006. Development of experimental setup for distinction of disease plant. ASABE Paper No. 063016. St. Joseph, Mich.: ASABE.

Qin, J., T. F. Burks, M. A. Ritenour, and G. W. Bonn. 2008. Detecting citrus canker by hyperspectral reflectance imaging and spectral information divergence. ASABE Paper No. 084066. St. Joseph, Mich.: ASABE.

Tian, Y., Ke, S. and Ke, C. 1996. Polymerase chain reaction for detection and quantization of Liberobacter asiaticum, the bacterium associated with Huanglongbing (Greening) of citrus in China. Proceedings of 13th Conference of the International Organization of Citrus Virologists (IOCV), University of California, Riverside, USA, 1996, pp. 252–257.

USDA APHIS. 2009. Citrus greening summit findings and national plan development. www.aphis.usda.gov/plant_health/plant_pest_info/citrus_greening. Accessed February 2009.

Yang, C. 2010. An airborne four-camera imaging system for agricultural applications. ASABE Paper No. 1008855, ASABE, St. Joseph, Michigan.

Yang, C., J. H. Everitt, M. R. Davis, and C. Mao. 2003. A CCD camera-based hyperspectral imaging system for stationary and airborne applications. Geocarto International Journal 18(2): 71-80.

Yang, C. 2009. Assessment of the severity of bacterial leaf blight in rice using canopy hyperspectral reflectance. Precision Agriculture Journal:DOI 10.1007/s11119-009-9122.

Ye, X., K. Sakai, S. Asada, and A. Sasao. 2007. Use of airborne multispectral imagery to discriminate and map weed infestations in a citrus orchard. *Weed Biology and Management* 7:23-30.